Skew Mu Toolbox (SMT): a presentation

G. Ferreres and J-M. Biannic
ONERA-CERT / DCSD
BP 4025, F-31055 Toulouse Cedex 4
ferreres@cert.fr, biannic@cert.fr

August 2003

Abstract

The aim of this freeware is to provide computational μ and skew μ methods for analysing the robust stability and performance properties of an uncertain closed loop, subject to LTI parametric uncertainties, neglected dynamics and to some extent uncertain time-delays. It could also be considered as a software complement to the book in [5] (G. Ferreres, A practical approach to robustness analysis with aeronautical applications, Kluwer Academic/Plenum Publishers, 1999). This toolbox includes basic routines to compute upper and lower bounds of classical but also skew μ, for both complex and real uncertainties. Several types of algorithms (exponential-time and polynomial-time) are made available. Unlike most other available robustness analysis tools, this toolbox also contains fully automated procedures which allows a non specialist to obtain guaranteed stability or performance robustness margins. Finally, different realistic engineering applications are included (missile, rigid and flexible aircraft, telescope mock-up), which illustrates the efficiency and the reliability of the proposed tools.

Available on the web pages http://www.cert.fr/dcsd/idco/perso/Biannic/mypage.html and http://www.cert.fr/dcsd/idco/perso/Ferreres/index.html

1 Introduction

Acronyms: LHP (Left Half Plane), LFR (Linear Fractional Representation), LFT (Linear Fractional Transformation), LTI (Linear Time Invariant), RHP (Right Half Plane), s.s.v. (structured singular value).

The aim of this freeware is to provide computational μ and skew μ methods for analysing the robustness properties of an uncertain closed loop, subject to LTI parametric uncertainties, neglected dynamics and uncertain time-delays. Consider a closed loop subject to different model uncertainties, and assume that the nominal closed loop (i.e. without model uncertainties) is asymptotically stable or more generally satisfies a stability or performance criterion. The issue is to estimate the robustness margin, i.e. the maximal amount of model uncertainties for which the closed loop is stable or satisfies this criterion.

Since the introduction of μ at the beginning of the Eighties [3, 13], the s.s.v. μ and its extensions, especially skew μ, have proven to be efficient tools for solving such problems, as testified by realistic engineering applications (see e.g. [5] and included references, as well as the applicative examples of this toolbox).

Nevertheless many μ based techniques, which were proposed in the litterature, are not yet available as reliable computational tools. This software represents our own effort to bring some of these techniques from theory into reality. This especially concerns different works in [2, 1] and techniques described in [5], which gathers different works in [8, 6, 7, 9] (the list is not exhaustive). As a matter of fact this toolbox could also be considered as a software complement to [5].

Note that extensive tests were performed[1], so that this software should be rather reliable. Nevertheless unavoidable bugs are still possible, please report them to the authors if you encouter one (or more!).

As a first step before the application of robustness tools the open loop plant model, with uncertainties in its physical parameters, must be put under a standard LFT form. We suppose in this toolbox that this LFT form was already computed, using e.g. the free LFR Toolbox in [10]. Finally a few words about the limitations of the Skew Mu Toolbox:

- This software only deals with robustness analysis problems, the robust control design problem is not considered here.
- Only the case of continuous-time systems is dealt with, and the closed loop and model uncertainties are supposed to be LTI. The case of time-varying and/or nonlinear model uncertainties is not accounted for.

[1] Even if our applicative examples essentially deal with non-repeated parametric uncertainties tests were performed using different structures of Δ, including the case of real, complex and mixed model perturbations, and the case of repeated real and complex scalars.

- The LMI Control Toolbox is required as an LMI solver, as well as the basic Control System Toolbox (and Simulink to some extent). No other toolbox is a priori necessary, especially the μ Analysis and Synthesis one, even if this toolbox can reveal useful in some situations: our methods for computing μ bounds may be less efficient than the ones proposed in this toolbox, noting that the μ Analysis and Synthesis Toolbox only deals with classical μ problems, not skew μ ones. See section 5.1 for more details. Other μ tools can also be found in the Robust Control Toolbox and in the LMI Control Toolbox.

Despite the above limitations our sofware should prove to be useful in many practical examples, and different extensions are forecast in future versions.

2 Implementation of the toolbox

The implementation of the toolbox should be very easy. No compilation of mex file is required, just *.m files are used:

- Just type "unzip SMT.zip" to unzip the downloaded file. A directory SMT will be created.
- Go to this directory and launch Matlab.
- Launch $first\_thing\_to\_do.m$, and then $demo\_mu.m$ or $demo\_skew\_mu.m$ for demos. This function will ask whether the μ Analysis and Synthesis Toolbox is available on the computer.

3 Technical preliminaries

This section introduces the μ framework. See [5] for a more detailed presentation.

3.1 the standard interconnection structure M - Δ

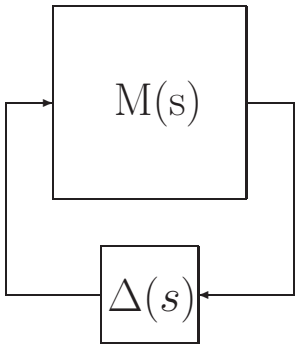

Figure 1: Standard interconnection structure.

The starting point of this toolbox is the standard interconnection structure $M(s)$ - $\Delta(s)$ of figure 1, see [5] for the obtention of such a structure. Consider indeed an LTI closed loop subject to parametric uncertainties and neglected dynamics. It is most generally possible to transform a specific uncertain closed loop into this standard interconnection structure: the transfer matrix $M(s)$ contains the dynamics of the nominal closed loop (i.e. the closed loop without any model uncertainty) and the way the various model perturbations enter the closed loop. On the other hand, all model perturbations are gathered in the uncertain transfer matrix $\Delta(s)$, which has the following block diagonal structure:

$$\Delta(s) = diag(\Delta_1(s), \ldots, \Delta_m(s), \delta_1 I_{q_1}, \ldots, \delta_n I_{q_n}) \tag{1}$$

$\Delta(s)$ is called a structured model perturbation. $\Delta_i(s)$ is a block of neglected dynamics wich is assumed to satisfy the H_∞ constraint:

$$\|\Delta_i(s)\|_\infty \leq 1 \tag{2}$$

δ_i is a real parametric uncertainty which is assumed to satisfy $\delta_i \in [-1,\ 1]$. These model uncertainties are obviously normalized. A template $W(s)$ is specified, so that the true neglected dynamics is $W(s)\Delta(s)$, while the uncertain parameter is $p = p^0 + \alpha\delta$. p^0 is the nominal value, and α is a weighting factor. If e.g. $\alpha = 0.1$, $\delta \in [-1,\ 1]$ means that p varies between $\pm$ 10 %.

Since the poles of $M(s)$ coincide with the poles of the nominal closed loop $M(s)$ is assumed to be asymptotically stable (no pole on the RHP or even on the imaginary axis). let $B\Delta(s)$ the unit ball:

$$B\Delta(s) = \{\Delta(s) \ \mid \ \|\Delta(s)\|_\infty < 1\} \tag{3}$$

This means that all blocks of neglected dynamics satisfy (2) and all $\delta_i \in [-1,\ 1]$. The robustness margin k_m is defined as the maximal amount of model uncertainties, for which the closed loop

is stable, i.e. the maximal value of k for which the closed loop of figure 1 (and thus the original uncertain closed loop which was put under such a standard form) is stable for all $\Delta(s) \in kB\Delta(s)$. In the μ context the robustness margin k_m is computed as:

$$k_m = \frac{1}{\max_{\omega\in[0,+\infty)} \mu(M(j\omega))} \tag{4}$$

$\mu(M(j\omega))$ is the s.s.v. associated to complex matrix $M(j\omega)$ and to structure (1) of the model perturbation. Note finally that a block of neglected dynamics $\Delta_i(s)$ becomes a full complex block at frequency ω, and that constraint (2) becomes at this frequency:

$$\overline{\sigma}(\Delta_i(j\omega)) \leq 1 \tag{5}$$

3.2 Definition of μ

The ω dependence is left out in the following: the complex matrix M represents the value of the transfer matrix $M(s)$ at $s = j\omega$, while the model perturbation Δ is an uncertain complex matrix, which also represents the value of the uncertain transfer matrix $\Delta(s)$ at $s = j\omega$.

A mixed structured perturbation Δ is a free complex matrix with the following specific structure:

$$\Delta = diag(\delta_1^r I_{k_1}, \ldots, \delta_{m_r}^r I_{k_{m_r}}, \delta_1^c I_{k_{m_r+1}}, \ldots, \delta_{m_c}^c I_{k_{m_r+m_c}}, \Delta_1^C, \ldots, \Delta_{m_C}^C) \tag{6}$$

With classical notations [4], Δ contains real scalars δ_i^r (which represent the parametric uncertainties), complex scalars δ_j^c and full complex blocks $\Delta_q^C \in C^{k_{m_r+m_c+q}, k_{m_r+m_c+q}}$ (which typically represent the neglected dynamics). The integers m_r, m_c, m_C and k_i define the structure of the perturbation. A real scalar $\delta_i^r I_{k_i}$ (resp. a complex scalar $\delta_i^c I_{k_{m_r+i}}$) is said to be repeated if the integer k_i (resp. k_{m_r+i}) is strictly greater than one.

Δ is said to be a *complex* model perturbation if it only contains complex scalars and full complex blocks. Conversely, Δ is a *real* model perturbation if it only contains real scalars. Δ is finally a *mixed* model perturbation when it simultaneously contains real and complex uncertainties.

The unit ball $B\Delta$ is introduced in the space of the structured perturbation Δ:

$$B\Delta = \{\Delta \ / \ \overline{\sigma}(\Delta) \leq 1\} \tag{7}$$

The *s.s.v.* is now defined as:

$$\begin{aligned} \mu_\Delta(M) &= 1/min(k \ / \ \exists \Delta \in kB\Delta \ with \ det(I - M\Delta) = 0) \\ &= 0 \ if \ no \ (k, \Delta) \ exists \end{aligned} \tag{8}$$

Remarks:
(*i*) The notation $\mu_\Delta(M)$ indicates that this value simultaneously depends on complex matrix

M and on the structure of the model perturbation Δ. For the sake of simplicity, we will often drop out the Δ dependence, *i.e.* simply note $\mu(M)$.
(*ii*) The singularity of matrix $I - M(j\omega_0)\Delta$ indicates the presence on the imaginary axis at $j\omega_0$ of a pole of the standard interconnection structure $M(s) - \Delta$. In this context, with reference to equation (4), the robustness margin, initially defined as the maximal amount of model uncertainties, for which the closed loop poles remain inside the LHP, can be reinterpreted as the size of the smallest destabilizing model perturbation, i.e. the one which brings one closed loop pole on the imaginary axis, i.e. on the border of the LHP.

3.3 Definition of the skew s.s.v. ν

Δ is now split as $\Delta = diag(\Delta_1, \Delta_2)$, where Δ_1 and Δ_2 are two mixed structured perturbations. M is partitioned in the same way as:

$$M = \begin{bmatrix} M_{11} & M_{12} \\ M_{21} & M_{22} \end{bmatrix} \tag{9}$$

The skew *s.s.v.* $\nu(M)$ is defined as:

$$\begin{aligned} \nu(M) &= 1/min(k \;/\; \exists \Delta = diag(\Delta_1, k\Delta_2) \; with \; \Delta_i \in B\Delta_i \\ &\qquad\qquad\qquad\qquad and \; det(I - M\Delta) = 0) \\ &= 0 \; if \; no \; (k, \Delta_1, \Delta_2) \; exists \end{aligned} \tag{10}$$

When computing μ, the unit ball $B\Delta$ is expanded (or shrunk) by factor k until the matrix $I - M\Delta$ becomes singular for a structured perturbation inside $kB\Delta$. When computing ν, the unit ball $B\Delta_2$ (in the space of perturbations Δ_2) is expanded (or shrunk) by factor k, but the structured perturbation Δ_1 remains now inside its unit ball $B\Delta_1$.

Remark: $\nu(M)$ takes an infinite value if and only if $\mu_{\Delta_1}(M_{11}) \geq 1$. This means that there exists Δ_1 with $\overline{\sigma}(\Delta_1) \leq 1$ and $det(I - Mdiag(\Delta_1, 0)) = 0$, or equivalently $det(I - M_{11}\Delta_1) = 0$.

3.4 Robust performance problems

Performance can be defined in two different ways. In the case of a real model perturbation, a first solution is to study the robustness of the location of the closed loop poles despite parametric uncertainties. In the general context of a mixed model perturbation, a second and more classical solution consists in checking whether a frequency domain template on a closed loop transfer matrix remains satisfied despite model uncertainties. In the first issue, performance is rather defined in the time domain, whereas performance is defined in the frequency domain in the second one.

3.4.1 Ω stability

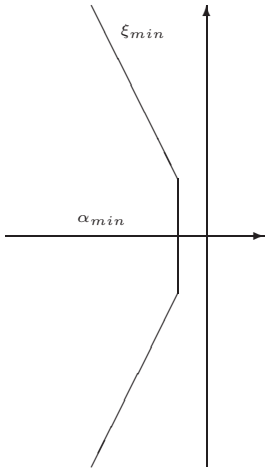

Figure 2: Robustness of a pole placement.

In the case of a real model perturbation, it is possible to study the robustness of the location of the closed loop poles in other regions than the LHP. This is especially the case of a truncated sector (see figure 2). Performance can be defined in this context by minimal values ξ_{min} and α_{min} for the damping ratio ξ and the degree of stability α [2]. To some extent, these specifications correspond to requirements on the rise time and overshoot of the closed loop step response, or on the time needed to reject an unmeasured disturbance or a non zero initial condition.

In this context the robustness margin, defined as the maximal amount of model uncertainties for which the closed loop poles remain inside the truncated sector, can still be computed with a frequency domain approach (4). But the s.s.v. is computed on the border of the truncated sector, instead of the border of the LHP, i.e. the imaginary axis.

Remarks:
(i) Nominal closed loop poles (i.e. those of $M(s)$) must belong to the truncated sector.
(ii) Neglected dynamics are undefined outside the imaginary axis.

[2] the degree α of stability of a state matrix A is defined as $\alpha = \max_i Re(\lambda_i(A))$, where $\lambda_i(A)$ is an eigenvalue of A.

3.4.2 H_∞ performance

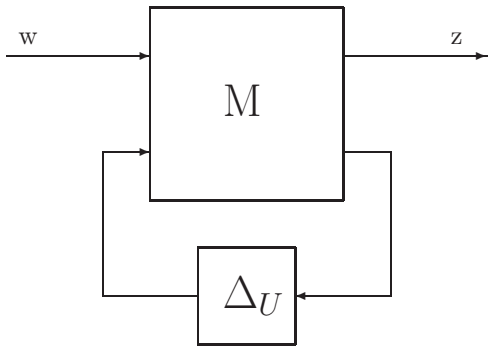

Figure 3: Augmented μ problem for robust performance analysis.

In the spirit of H_∞ control, performance is achieved if a closed loop transfer matrix $T(s)$ satisfies a frequency domain template $W(s)$ at all frequencies ω:

$$\overline{\sigma}(W(j\omega)T(j\omega)) < 1 \tag{11}$$

Assume now the presence of uncertainties in the closed loop, so that $T(s)$ is an LFT:

$$T(s) = F_l(M(s), \Delta_U(s))$$

(*i.e.* the transfer between w and z in figure 3). $\Delta_U(s)$ is most generally a mixed model perturbation, containing parametric uncertainties and neglected dynamics. Assume moreover that $W(s)$ is included in $F_l(M(s), \Delta_U(s))$ to alleviate the notations.
The nominal closed loop is assumed to satisfy the performance property at ω, *i.e.* :

$$\overline{\sigma}(F_l(M(j\omega), 0)) < 1 \tag{12}$$

The robust performance problem consists in computing the maximal amount of uncertainties, for which closed loop performance is still achieved. The problem is thus to compute the maximal size of the mixed model perturbation $\Delta_U(j\omega)$, for which the following relation remains satisfied:

$$\overline{\sigma}(F_l(M(j\omega), \Delta_U(j\omega))) < 1 \tag{13}$$

Here again the problem is solved at each frequency ω. This robust performance problem can be equivalently transformed into an augmented robust stability problem, involving an additional fictitious full complex block (which is called a fictitious performance block) Δ_P. On figure 3 Δ_P is connected to the inputs and outputs w and z, so that the standard interconnection structure of figure 1 is obtained with $\Delta = diag(\Delta_P, \Delta_U)$. Computing the maximal amount

of uncertainties, for which closed loop performance is achieved is a skew μ problem in which the fictitious performance block Δ_P is maintained inside its unit ball while the size of the model perturbation Δ_U is maximised.

Remark: the performance block Δ_P can be structured. Assume that $F_l(M, \Delta_U)$ is a Two Inputs Two Outputs transfer matrix, and we are just interested in both direct SISO transfer functions (i.e. the transfer function between the 1st input and output, and the transfer function between the 2d input and output). In order to find the worst-case simultaneous degradation of the performance on these 2 transfer functions just choose $\Delta_P = diag(\delta_1^c, \delta_2^c)$, where each δ_i^c is a complex scalar.

3.5 Computational difficulties

• A common practice for solving (4) is to compute the *s.s.v.* $\mu(M(j\omega))$ at each point of a frequency gridding $(\omega_i)_{i\in[1,N]}$. When choosing a sufficiently fine frequency gridding, good results are obtained in many practical examples. Nevertheless a specific problem appears in the context of flexible systems: narrow and high peaks may indeed be obtained on the plot of $\mu(M(j\omega))$ as a function of frequency ω. The use of a frequency gridding reveals unreliable in such a case: the risk is to miss a narrow and high peak on the μ plot, and thus to overevaluate the robustness properties of the closed loop (by underevaluating the value of the maximal *s.s.v.* over the frequency range). In the context of this new and difficult problem, we propose in section 5.2 two methods for computing a reliable estimate of $\mu(M(j\omega))$ as a function of ω.

• Computing the exact value of the *s.s.v.* is an NP hard problem, so that the computational burden of the algorithms, which compute the exact value of μ, is necessarily an exponential function of the size of the problem. It is consequently impossible in practice to compute the exact value of μ for large dimension problems. A usual solution is to compute μ upper and lower bounds instead of the exact value. The associated algorithms can be exponential-time (like the algorithms which compute the exact value of μ), or more interestingly polynomial-time. Even if it is not possible to guarantee a priori the gap between the μ bounds when using polynomial-time algorithms, good results are usually obtained in practical realistic examples: this will be illustrated in the following.

• From a computational point of view, a (skew) μ upper bound is typically obtained as the solution of a convex or quasi-convex optimization problem, namely an LMI problem. Conversely, the methods which compute a μ lower bound are generally heuristic, and the computational burden is typically required to be low. The most classical solution consists in solving in an heuristic way a non convex optimisation problem: indeed a μ lower bound typically corresponds to a local optimum of this non convex optimisation problem, whereas the exact value of μ corresponds to the global optimum of this optimisation problem.

• The pratical usefulness of the μ bounds is now explained. For the sake of clarity, we restrict our attention to the case of a real model perturbation $\Delta = diag(\delta_i I_{q_i})$. Let D the unit hypercube:

$$D = \{\delta = [\delta_1 \dots \delta_n] \mid \delta_i \in R \; and \; |\delta_i| \leq 1\} \tag{14}$$

D corresponds to the unit ball in the specific context of a real model perturbation. An upper bound $\overline{\mu}$ of $\mu(M)$ gives a sufficient condition of nonsingularity of the matrix $I - M\Delta$, which is thus guaranteed to be nonsingular for all parametric uncertainties Δ inside $(1/\overline{\mu})D$. An *upper bound* $\overline{\mu}$ of the *s.s.v.* thus gives a *lower bound* k_L of the robustness margin:

$$k_L = \min_{\omega \in [0,\, \infty)} \frac{1}{\overline{\mu}(M(j\omega))} \tag{15}$$

In the context of a robust stability problem in the presence of parametric uncertainties, robust stability of the closed loop can thus be guaranteed inside the hypercube $k_L D$ in the space of uncertain parameters.

Conversely, a lower bound $\underline{\mu}$ of $\mu(M)$ gives a sufficient condition of singularity of the matrix $I - M\Delta$, i.e. there exists a real model perturbation $\Delta^* \in (1/\underline{\mu})D$, with $I - M\Delta^*$ singular (in the context of a robust stability problem, Δ^* is a destabilizing model perturbation). The usefulness of a μ lower bound is twofold. As a first point, $\underline{\mu}$ gives a measure of the conservatism of the upper bound $\overline{\mu}$, by examining the tightness of the interval $[\underline{\mu},\, \overline{\mu}]$ which contains the exact value of μ. As a second point, an associated *worst-case* model perturbation Δ^* is usually provided with $\underline{\mu}$ by the computational algorithm.

4 Content of the toolbox

4.1 Applicative examples

The toolbox contains the following complementary applications:

- De Gaston and Safonov's example [2]: this very simple example only contains 3 non-repeated parametric uncertainties, and the order of $M(s)$ is 3. It is especially useful for a demo since the application of our μ tools is (very) fast on it.
- Longitudinal missile [12]: the structured model perturbation Δ contains 4 non-repeated parametric uncertainties, a block of neglected dynamics and a performance block. The order of $M(s)$ is 19. Simpler sub-problems can be considered (e.g. only with parametric uncertainties), see the following subsection. See also section 12 for the computation of worst-case MIMO gain, phase and delay margins in the presence of the 4 non-repeated parametric uncertainties.

- Lateral rigid airplane [5]: the structured model perturbation Δ contains 14 non-repeated parametric uncertainties, and the order of $M(s)$ is 9. In all above 3 examples μ bounds can be computed on a frequency gridding. But in the case of the lateral rigid airplane, the large number of parametric uncertainties prohibits the use of exponential-time methods.
- Lateral rigid + flexible airplane [5]: the structured model perturbation Δ contains 20 non-repeated parametric uncertainties, and the order of $M(s)$ is 46. Because of the flexible model it becomes difficult to compute μ bounds on a frequency gridding.
- Telescope mock-up [5]: the structured model perturbation Δ contains 20 non-repeated parametric uncertainties, and the order of $M(s)$ is 70. Because of the highly flexible model it becomes impossible to compute μ bounds on a frequency gridding. A challenging problem when considering the large number of parametric uncertainties and the order of $M(s)$.

All examples above correspond to robust stability problems (inside the LHP or truncated sector), except the missile example which also contains a robust performance problem. More details on these applications can be found in [5] and included references (see also the README file in the directory Applications). We detail in the following subsection the missile problem.

4.2 More on the missile example

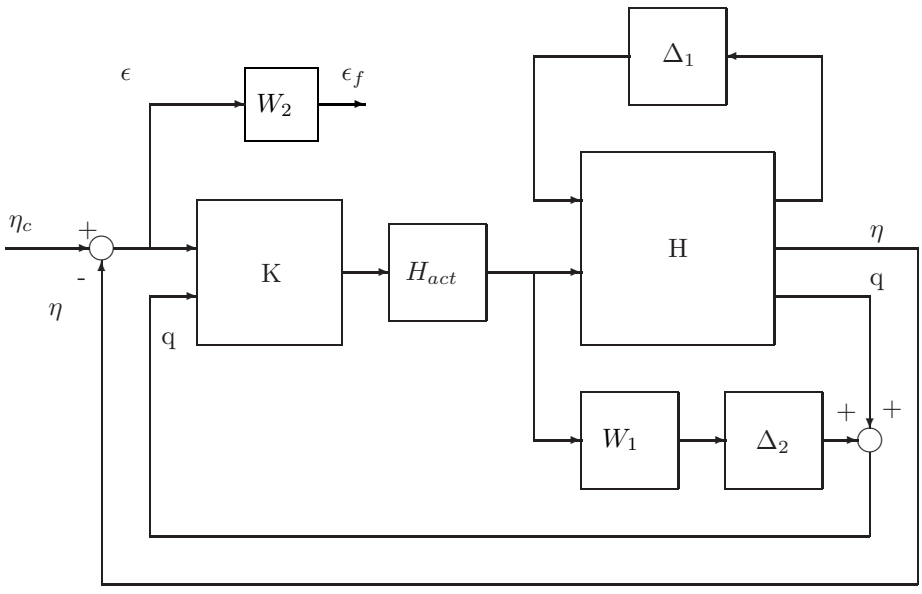

Figure 4: Closed loop missile system with uncertainties.

The issue is to analyse the stability and performance properties of the closed loop missile in the presence of uncertainties in its 4 physical parameters and in the face of neglected dynamics, namely a high frequency bending mode. To this aim, the parametrically uncertain missile model was first transformed into the standard LFT structure $F_u(H(s), \Delta_1)$, where Δ_1 gathers the parametric uncertainties. On the other hand, the bending mode is represented by an additive model perturbation $\Delta_2(s)$ and its template $1/W_1(s)$ is extracted from [12]. The uncertain closed loop missile is presented in figure 4, where $K(s)$ represents the feedback controller and $H_{act}(s)$ the actuator. Two outputs η and q are used by $K(s)$. In the context of H_∞ control, the frequency domain performance is finally defined through the sensitivity function S, *i.e.* the transfer function between the commanded acceleration η_c and the tracking error $\epsilon = \eta_c - \eta$. A frequency domain template $1/W_2(s)$ is to be satisfied, i.e. performance is obtained if the H_∞ norm of the transfer function between the commanded acceleration η_c and the filtered tracking error ϵ_f is less than 1.

4.3 Computational methods

	M or $M(s)$	μ or skew μ	LHP or sector	μ lower or up. bound	real, complex or mixed	polynomial or exp. time
mu_lb_with_freq.m	$M(s)$	μ	sector	lower	real	polynomial
mu_max_1.m	$M(s)$	skew μ	LHP	upper	mixed	polynomial
mu_max_2.m	$M(s)$	skew μ	LHP	upper	mixed	polynomial
mixed_mu_lb_freq.m	$M(s)$	skew μ	sector	lower	mixed	polynomial
mixed_mu_lb.m	M	skew μ	sector	lower	mixed	polynomial
mixed_mu_ub.m	M	skew μ	sector	upper	mixed	polynomial
mu_dailey.m	M	skew μ	sector	lower	real	exponential
mu_zd.m	M	skew μ	sector	upper	real	exponential
worst_case_margin.m	$M(s)$	skew μ	LHP	upper	mixed	polynomial

Table 1: characteristics of the (skew) μ methods.

In a few words, the toolbox contains the following computational methods for μ:

- With a frequency gridding: classical mixed μ lower and upper bounds (*mixed_mu_ub.m*, *mixed_mu_lb.m*), exponential-time real μ upper and lower bounds (*mu_zd.m*, *mu_dailey.m*). All these routines can also be called via *mu_frequency_gridding.m*. See also the function *mixed_mu_lb_freq.m*.

- Computation of a guaranteed (skew) mixed μ upper bound on a frequency interval: *mu_max_1.m* and *mu_max_2.m*.

- Computation of a real μ lower bound with a mixed frequency/state-space approach: $mu\_lb\_with\_freq.m$.
- With a frequency gridding, computation of worst-case values of MIMO gain, phase and delay margins in the presence of parametric uncertainties and neglected dynamics: $worst\_case\_margin.m$. See section 12 for more details.

$demo\_mu.m$ and $demo\_skew\_mu.m$ essentially call $robust.m$, which is an interactive interface to $mu\_frequency\_gridding.m$, $mu\_lb\_with\_freq.m$, $mu\_max\_1.m$ and $mu\_max\_2.m$. Noting that these routines can also be independently called. The table above summarizes the characteristics of the (skew) μ methods. M (resp. $M(s)$) means that the input argument of the routine is a complex matrix M (resp. a dynamic transfer matrix $M(s)$). μ means that the routine only deals with classical μ problems, while skew μ means that the routine deals with classical and skew μ problems. In the same way LHP means that the routine only deals with robust stability problems inside the LHP, while sector means that the routine deals with robust stability problems inside the LHP and truncated sector. Finally real, complex and mixed refer to the nature of the structured model perturbation.

4.4 Important details

4.4.1 description of the structure of Δ

The structure of Δ is described by blk. The first two colums of blk follow the format of the μ Analysis and Synthesis Toolbox. Each line of blk describes a component of Δ, i.e. a block of neglected dynamics, a (repeated) complex scalar or a (repeated) real scalar:

- If blk(i,1:2)=[n m], where n and m are strictly positive integers, this means that the ith block of Δ is a block of neglected dynamics, whose size is (n,m).
- If blk(i,1:2)=[n 0], where n is a strictly positive integer, the ith block of Δ is a repeated complex scalar δI_n.
- If blk(i,1:2)=[-n 0], where n is a strictly positive integer, the ith block of Δ is a repeated real scalar δI_n.

blk(i,1:2)=[-n m], where n and m are strictly positive integers, is not allowed (it would correspond to a full real block). The third column of blk describes the potentially skew nature of the uncertainty. If blk(i,3)=0 the ith block must be maintained inside the unit ball. If blk(i,3)=1 its size is free.

Note finally that M and Δ are supposed to be square in the interconnection

structure M - Δ. But a rectangular block of neglected dynamics can be encountered. In this context the interconnection structure M - Δ can be transformed into a new one, M_2 - Δ_2, where M_2 and Δ_2 are square. The idea is just to add zero lines or columns in M. This is automatically done with the routine $square\_m.m$.

4.4.2 choice of the frequency gridding

The choice of the frequency gridding, on which μ bounds are computed, is not especially complex, but it is user-dependent. The issue is just not to miss a critical μ peak. This gridding usually consists of the zero frequency and of N logarithmically spaced points between ω_{min} (a non-zero value) and ω_{max}. ω_{min} (resp. ω_{max}) should correspond to a very low (resp. very high) frequency. These obviously depend on the nature of the closed loop plant. As an example, since a missile is much faster than a transport airplane, ω_{max} can be chosen as 100 rad/s for the airplane, but 1000 for the missile. It can be worthwhile to inspect the frequencies of the nominal closed loop poles in order to determine ω_{min} and ω_{max}.

5 Some information on computational methods

This section gives some information on the computational methods. See the included references for more details.

5.1 Computation of the mixed μ lower and upper bounds

Concerning the computation of a mixed μ lower bound, our toolbox implements the original power algorithm in [14] (see [5] for the extension of this power algorithm to skew μ problems). The idea is to solve an equation $x = f(x)$ with power iterations, i.e. to look for the limit of $x_{k+1} = f(x_k)$. *If the algorithm converges*, a μ lower bound is obtained. Moreover the limit depends on the value of x_0. The original power algorithm in [14] was improved, see especially [11], but these improvements are not implemented in our software, so that our power algorithm is not as efficient as the power algorithm in the μ Analysis and Synthesis Toolbox. It shoud be noted however, that the latter does not handle skew μ problems, unlike ours.Note also that both power algorithms generally fail to converge in the presence of a purely real model perturbation, in which case the μ lower bound is taken as zero.

Concerning the computation of a mixed (skew) μ upper bound, our toolbox implements an LMI solution which uses the LMI solver of the LMI Control Toolbox (see [4] for the mixed μ upper bound and [8] for the extension to skew μ). Problems can be encountered with largely repeated real or complex scalars δI_n, since the number of scalar optimization parameters in the LMI grows as n^2, i.e. the computational burden can become cumbersome if n is too large.

A specific technique was developed in the μ Analysis and Synthesis Toolbox to reduce this computational burden in this context: the idea is to achieve a trade-off between the accuracy of the μ upper bound (i.e. its closeness to the minimal value, which would be provided by an LMI solver) and the computational burden.

Remarks:
(*i*) In our routines *mixed_mu_lb.m* and *mixed_mu_ub.m*, in the context of a classical μ problem, it is possible to call the routine *mu.m* (computation of a μ lower or upper bound, if the μ Analysis and Synthesis Toolbox is available on the computer) as well as the LMI Control Toolbox routine *mubnd.m* (computation of a μ upper bound). see the help of *mixed_mu_lb.m* and *mixed_mu_ub.m* for details.
(*ii*) Since the power algorithm in the μ Analysis and Synthesis Toolbox generally works better than ours, it is used in our toolbox whenever it is possible. Obviously, if the μ Analysis and Synthesis Toolbox is not available on the computer, our power algorithm is always used. Otherwise, the power algorithm in the μ Analysis and Synthesis Toolbox is used for all classical μ problems (in *mu_frequency_gridding.m* and *mu_lb_with_freq.m*), and our algorithm is used only for skew μ ones. Nevertheless, note that our power algorithm provides satisfactory results in the examples of section 11, where a mixed (skew) μ lower bound is to be computed on a frequency gridding. But our power algorithm is rather slower than the one in the μ Analysis and Synthesis Toolbox.
(*iii*) The convergence properties of our power algorithm are better in the case of a classical μ problem, than in the case of a skew μ one. This is due to the introduction of an additional scaling factor in the power algorithm, as explained in [5].

5.2 Computation of a guaranteed μ upper bound on a frequency interval

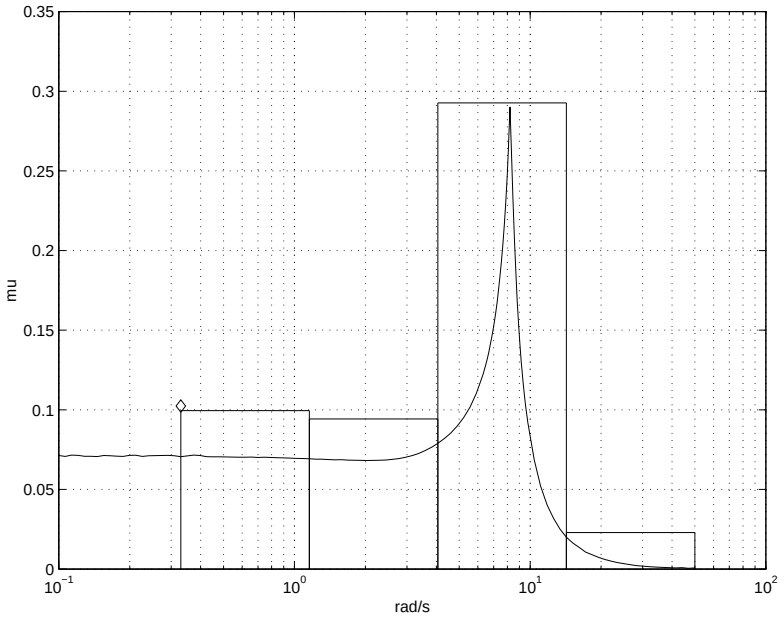

Figure 5: μ for De Gaston and Safonov's example.

In the context of flexible systems, a reliable robustness margin can be obtained by computing guaranteed μ upper bounds β_i on frequency intervals $[\omega_i,\ \omega_{i+1}]$, i.e. one can guarantee that:

$$\mu(M(j\omega)) \leq \beta_i \ \ \forall \omega \in [\omega_i,\ \omega_{i+1}] \tag{16}$$

It now becomes impossible to miss a μ peak, and a guaranteed upper bound of the maximal value of μ over the frequency range can be deduced. Two different methods are available in $mu\_max\_1.m$ [6, 9] and $mu\_max\_2.m$ [8]. Most generally, $mu\_max\_1.m$ provides less conservative results with a lower computational burden. Indeed, the initial frequency gridding is refined inside $mu\_max\_1.m$, i.e. μ peaks are automatically detected[3]. Moreover $mu\_max\_2.m$ solves a skew μ problem in which appears the repeated real scalar $\delta\omega I_n$, where $\delta\omega$ is the frequency (treated as an uncertainty) and n is the order of $M(s)$. Thus, as indicated in the above subsection, the computational burden can be very high if n is too large.

[3]In the context of the classical mixed μ upper bound (or its extension to skew μ), the issue is to compute D, G scaling matrices, which are valid at the two extremal frequencies, and to check a posteriori that these D, G scaling matrices are also valid inside the associated interval. If not the interval is split into two smaller intervals.

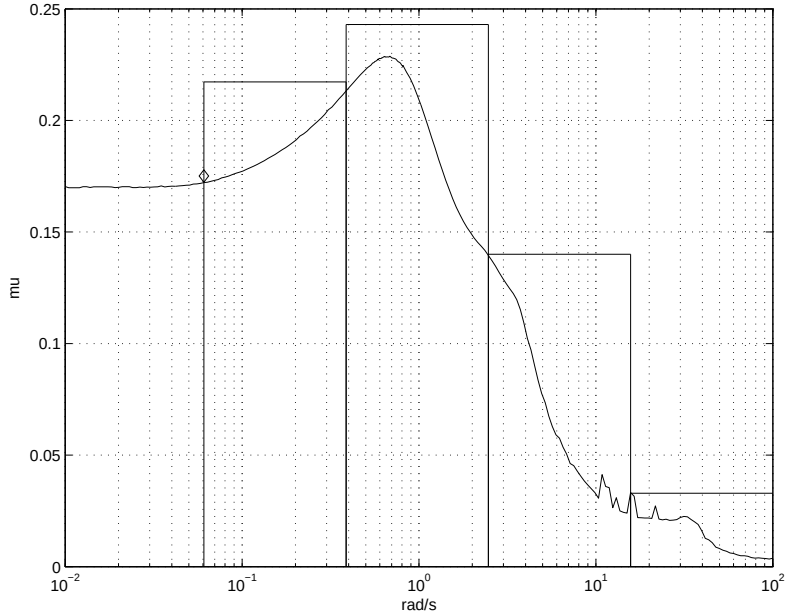

Figure 6: μ for the rigid aircraft example.

Note nevertheless that figure 5, which corresponds to De Gaston and Safonov's example, suggests that *mu_max_2.m* does not necessarily provide a μ upper bound, which is more conservative than the mixed μ upper bound computed with the function *mixed_mu_ub.m* on a fine frequency gridding (when it is possible to use such a gridding). Note indeed that the guaranteed μ upper bound on the critical frequency interval (i.e. the one corresponding to the maximal value of μ) nearly coincides with the maximal μ upper bound, computed on a frequency gridding, over the same interval. The same type of results is obtained on the rigid aircraft example: see figure 6.

Remarks:
(*i*) See the help of *mu_max_1.m* and *mu_max_2.m* and [8, 6, 5, 9] for more details.
(*ii*) These 2 routines only deal with robust stability problems inside the LHP. Indeed, robust stability inside a truncated sector appears useful for rigid systems, not for flexible ones.

5.3 Exponential-time real μ methods

mu_dailey.m and *mu_zd.m* propose methods for computing lower or upper bounds of μ at a given frequency in the special case of non-repeated real uncertainties. Since these methods are exponential-time their application is limited to about 10 or 12 uncertain parameters. Despite

all these limitations these methods are worthwhile in the context of a real μ problem with a limited number of uncertainties (see especially the missile application).

mu_dailey.m is an implementation of Dailey's method in [1], while *mu_zd.m* uses a Zero Exclusion Test combined with the Mapping Theorem [15], as initially proposed in [2] (note nevertheless that no branch and bound is implemented in *mu_zd.m*, the issue is just to compute a μ upper bound).

Remarks:
(*i*) At the zero frequency (and also at very low frequencies) *mu_dailey.m* willingly provides no result (because matrix $M(j\omega)$ is real, and not complex at the zero frequency). Conversely, *mu_zd.m* provides the exact value of μ at the zero frequency.
(*ii*) When using *mu_dailey.m*, if the μ lower bound is less than 1e-3 it is taken as zero. Conversely, when using *mu_zd.m*, if the μ upper bound is less than 1e-3 it is taken as 1e-3.

5.4 Computation of a μ lower bound with a mixed frequency/state-space approach

mu_lb_with_freq.m implements the method proposed in [7]. See the help of this routine for a presentation of the technique. Simply note that 4 related methods are proposed in *mu_lb_with_freq.m*, but the most valuable ones are the 2th and 4th ones, as indicated in section 8. Note also that only real parametric uncertainties are dealt with (no complex uncertainties), and only classical μ problems (no skew μ one). Indeed, the power algorithm in section 5.1 especially fails to converge in the context of a purely real model perturbation.

6 Introduction to the applicative sections

The following sections will present the computational methods through different applicative examples:

- (robust stability in the presence of 4 parametric uncertainties) The missile example only contains 4 parametric uncertainties, so that exponential-time methods can be used. It is possible to study robust stability inside the LHP or truncated sector.
- (robust stability in the presence of 14 parametric uncertainties) The rigid airplane contains 14 parametric uncertainties, so that only polynomial-time methods can be used now.
- (robust stability in the presence of 20 parametric uncertainties) The telescope mock-up example is highly flexible, so that it is no more possible to compute μ on a frequency gridding.

- Skew μ problems are illustrated on the missile example through 2 robust stability and performance problems.
- The last section explains on the missile example how to compute estimates of worst-case MIMO gain, phase and delay margins.

Note finally that *demo_mu.m* and *demo_skew_mu.m* can be used to compare methods in many other situations than the ones described above and below.

7 Missile: robust stability

Robust stability in the presence of the 4 parametric uncertainties is studied in this section, i.e. neither the neglected dynamics nor the performance block are considered here.

7.1 Robust stability in the LHP

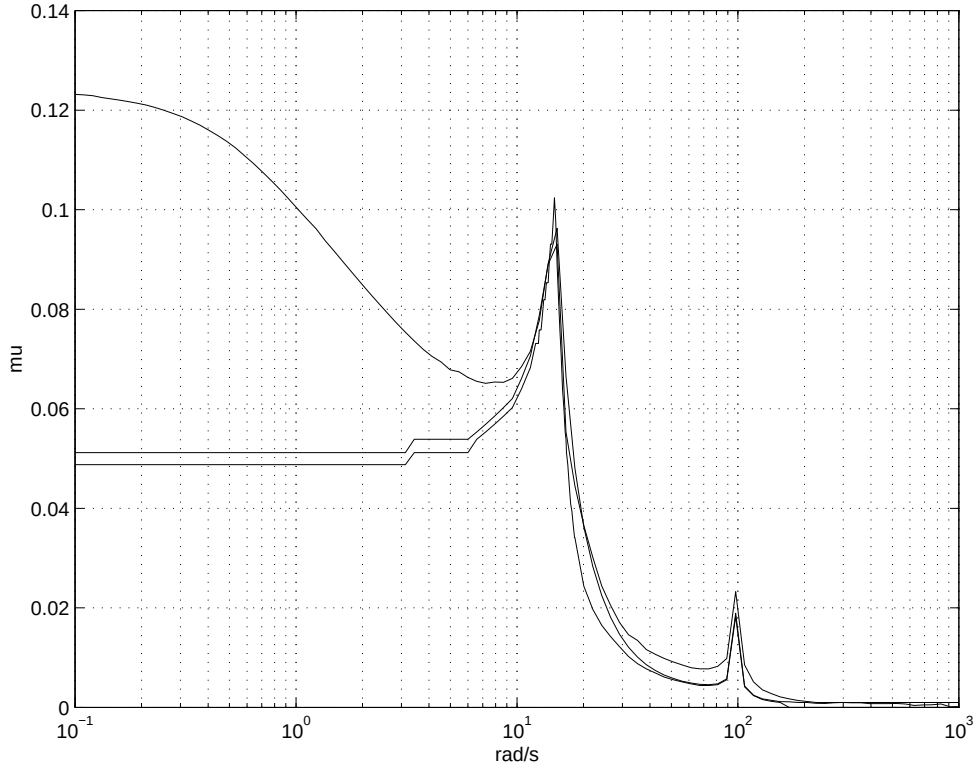

Figure 7: μ for the missile example (robust stability inside the LHP).

The above figure presents the results provided by *mixed_mu_ub.m* (mixed μ upper bound), *mu_zd.m* (exponential-time upper bound) and *mu_dailey.m* (exponential-time lower bound). Both upper bounds are close, except at low frequencies where the highest is the mixed μ upper bound. Noting moreover that both μ upper bounds are equal to 0.125 at the zero frequency. It can be concluded that μ is discontinuous at this frequency. The exponential-time lower and upper bounds are (very) close, so that the exact value of μ is around 0.05 at very low frequencies. But it is 0.125 at the zero frequency (the exponential-time upper bound coincides with the exact value at this specific frequency). Note moreover that the exponential-time upper

bound is discontinuous, but not the mixed μ upper bound. As a conclusion, at least in the case of a purely real model perturbation it is important to compute μ bounds at the zero frequency and at very low frequencies.

The maximal value of μ is 0.125 at the zero frequency, so that robust stability can be guaranteed for $\pm$ 40 % of uncertainty in the stability derivatives (i.e. the physical parameters of the missile model). Parametric uncertainties were indeed normalised by a weighting factor 0.05, so that the robustness margin is $\frac{0.05}{0.125}$.

7.2 Robust stability in a truncated sector

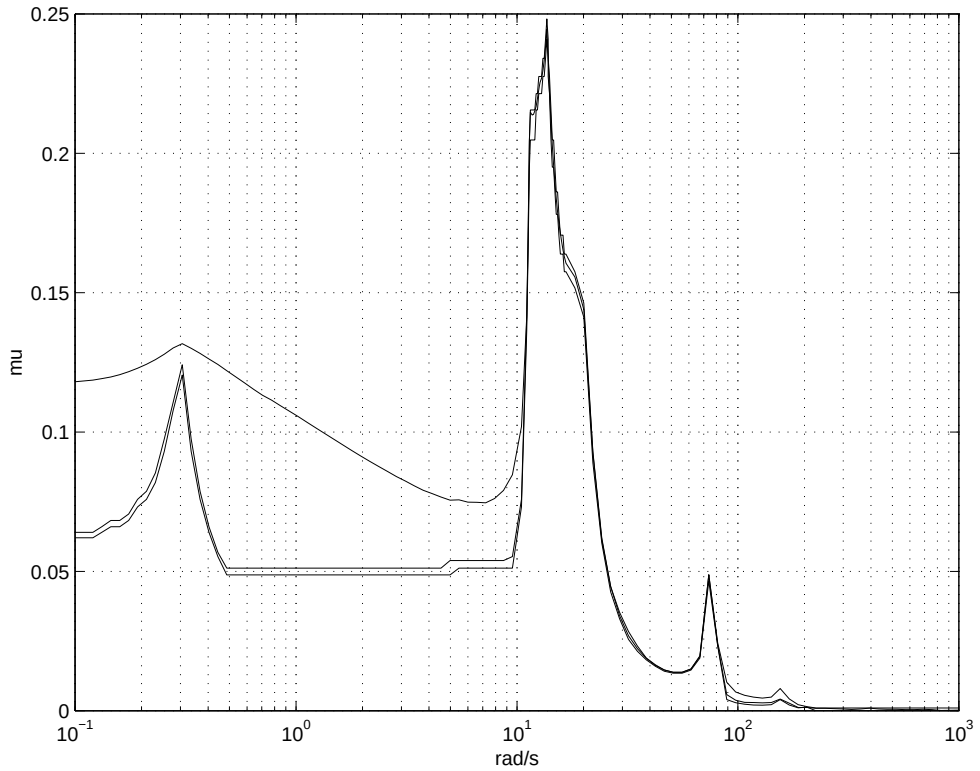

Figure 8: μ for the missile example (robust stability inside a truncated sector).

The poles of the nominal closed loop are:

Eigenvalue	Damping	Freq. (rad/s)
-4.94e-01	1.00e+00	4.94e-01
-5.00e-01	1.00e+00	5.00e-01
-7.55e+00	1.00e+00	7.55e+00
-7.56e+00 + 9.48e+00i	6.23e-01	1.21e+01
-7.56e+00 - 9.48e+00i	6.23e-01	1.21e+01
-2.60e+01 + 1.14e+01i	9.15e-01	2.84e+01
-2.60e+01 - 1.14e+01i	9.15e-01	2.84e+01
-1.16e+02	1.00e+00	1.16e+02
-9.43e+01 + 1.14e+02i	6.37e-01	1.48e+02
-9.43e+01 - 1.14e+02i	6.37e-01	1.48e+02
-1.04e+02 + 1.07e+02i	6.97e-01	1.49e+02
-1.04e+02 - 1.07e+02i	6.97e-01	1.49e+02
-1.80e+02 + 2.71e+01i	9.89e-01	1.82e+02
-1.80e+02 - 2.71e+01i	9.89e-01	1.82e+02

It is thus possible to study robust stability inside a truncated sector with -0.3 for the minimal degree of stability and 0.4 for the minimal damping ratio (remember the nominal closed loop poles must belong to the truncated sector).

In the above figure the same discontinuity problem appears at the zero frequency: μ is 0.123 at this frequency, and at low frequencies the highest bound is the mixed μ upper bound. Exponential-time lower and upper bounds are very close at all frequencies, and the maximal value of μ is computed with a nearly perfect accuracy: at the critical frequency 13.664 rad/s, the μ lower bound is 0.241 while the μ upper bounds are 0.245 and 0.248. This means that robust stability is guaranteed for $\pm$ 20 % of uncertainty in the stability derivatives ($0.2041 = \frac{0.05}{0.245}$).

8 Rigid airplane: robust stability in the LHP

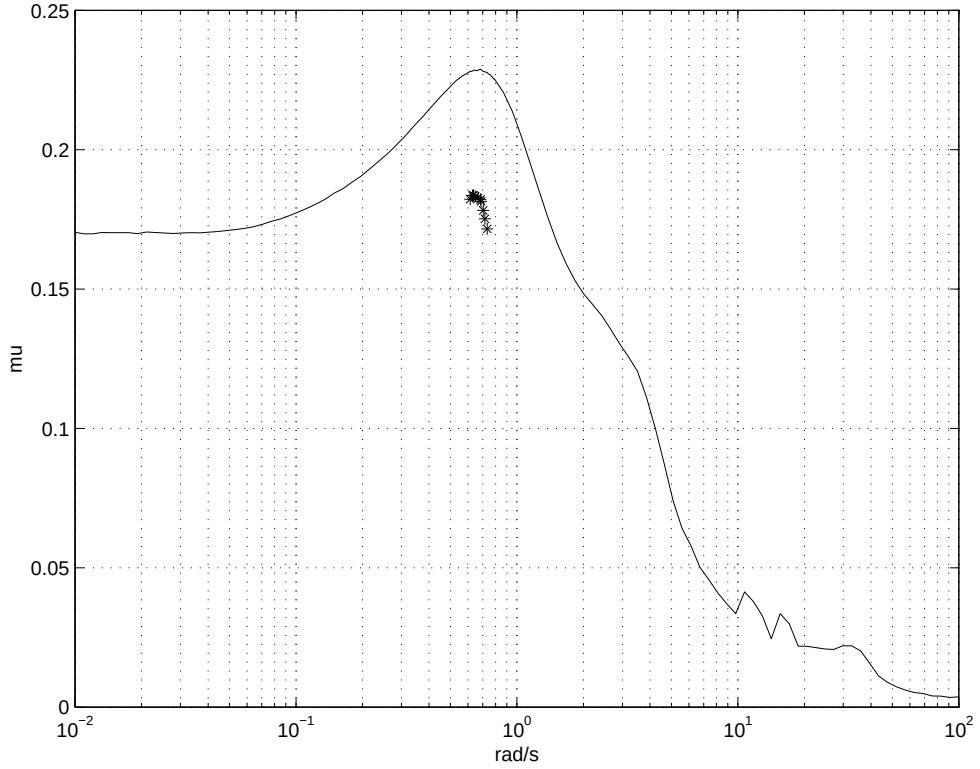

Figure 9: μ for the rigid airplane example (robust stability inside the LHP).

We consider 14 parametric uncertainties in the stability derivatives. When using a frequency gridding the sole method which can be used is now *mixed_mu_ub.m*. The power algorithm in *mixed_mu_lb.m* (which computes a mixed μ lower bound) generally provides no result in the context of a purely real model perturbation, and there are too many uncertainties for exponential-time methods in *mu_zd.m* and *mu_dailey.m*. The maximal value of the μ upper bound is obtained as:

```
Maximal value of mu =  0.229 at w =  0.687 rad/s
```

Since the weighting factor on the parametric uncertainties is 10 %, this means that robust stability is guaranteed for $\pm$ 44 % of uncertainty in the stability derivatives ($0.4367 = \frac{0.1}{0.229}$).

mixed_mu_lb_with_freq.m is then used to compute a μ lower bound. The aim of this routine is not to compute a μ lower bound as a function of frequency, but to compute a lower

bound of the maximal value of μ. This routine can be used in two different ways:

• If the μ upper bound was first computed as a function of frequency, then the potential conservatism can be evaluated by the routine *mixed_mu_lb_with_freq.m* which can be applied around the critical frequency, corresponding to the highest peak of the μ upper bound (here 0.68 rad/s). In this context the 4 possible methods in *mixed_mu_lb_with_freq.m* nearly give the same result:

```
Maximal value of mu =  0.184 at omega =  0.634 rad/s (method=1)
Maximal value of mu =  0.184 at omega =  0.623 rad/s (method=2)
Maximal value of mu =  0.179 at omega =  0.626 rad/s (method=3)
Maximal value of mu =  0.184 at omega =  0.634 rad/s (method=4)
```

The gap between the lower and upper bounds of the maximal value of μ over the frequency range is satisfactory (19 %). The stars on figure 9 represent the μ lower bounds.

• If nothing can be guessed about the critical frequency *mixed_mu_lb_with_freq.m* is applied on a large frequency interval, namely between 0.01 and 100 rad/s (and the zero frequency). In this new context the 4 possible methods in *mixed_mu_lb_with_freq.m* may give different results. To keep a low computational burden the number of frequency points is limited to 5 (frequencies are thus 0, 0.01, 0.1, 1, 10 and 100). Here is the result obtained with the 2d method:

```
1: reg. mu problem at    0.00 rad/s --> mu = 0.14  - imag. axis crossed at  0.00 rad/s
2: reg. mu problem at    0.01 rad/s --> mu = 0.14  - imag. axis crossed at  0.00 rad/s
3: reg. mu problem at    0.10 rad/s --> mu = 0.16  - imag. axis crossed at  0.33 rad/s
4: reg. mu problem at    1.00 rad/s --> mu = 0.18  - imag. axis crossed at  0.62 rad/s
5: reg. mu problem at   10.00 rad/s --> mu = 0.008 - imag. axis crossed at  6.99 rad/s
6: reg. mu problem at  100.00 rad/s --> mu = 0.018 - imag. axis crossed at 35.77 rad/s
```

A μ lower bound is obtained as a function of frequency (e.g. 0.14 at zero, or 0.16 at 0.33 rad/s), but note that these frequencies are not the same as the ones of the initial gridding. Thus, even if the initial rough frequency gridding does not contain the critical frequency, this one can be detected with our method. Here is the maximal μ lower bound obtained with the 4 methods:

```
Maximal value of mu =  0.144 at omega =  0.206 rad/s (method=1)
Maximal value of mu =  0.184 at omega =  0.623 rad/s (method=2)
Maximal value of mu =  0.135 at omega =  0.228 rad/s (method=3)
Maximal value of mu =  0.144 at omega =  0.206 rad/s (method=4)
```

The 2d method gives the best results, see [7] for an explanation. Note nevertheless that much better results are obtained when choosing 30 points between 0.01 and 100 rad/s (and the zero frequency):

```
Maximal value of mu =  0.183 at omega =  0.624 rad/s (method=1)
Maximal value of mu =  0.183 at omega =  0.623 rad/s (method=2)
Maximal value of mu =  0.178 at omega =  0.611 rad/s (method=3)
Maximal value of mu =  0.183 at omega =  0.624 rad/s (method=4)
```

Remarks:
(*i*) In some situations the 4th method gives better results than the 2d one.
(*ii*) It would be possible to study in the same way robust stability inside the truncated sector.
(*iii*) The above results were obtained using the power algorithm of the μ Analysis and Synthesis toolbox inside *mu_lb_with_freq.m*. If this toolbox is not available on the computer our power algorithm can be used, but the algorithm is slower and results are generally not as good as those obtained with the power algorithm of the μ Analysis and Synthesis toolbox. Here again, the most interesting methods are the 2d and 4th ones, and best results are obtained with the 2d or 4th method depending on the example.

9 Back to the missile example

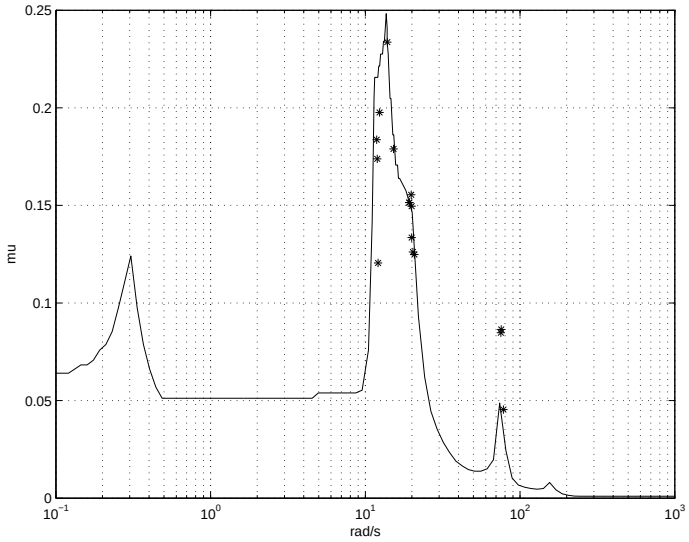

Figure 10: μ for the missile example (robust stability inside a truncated sector).

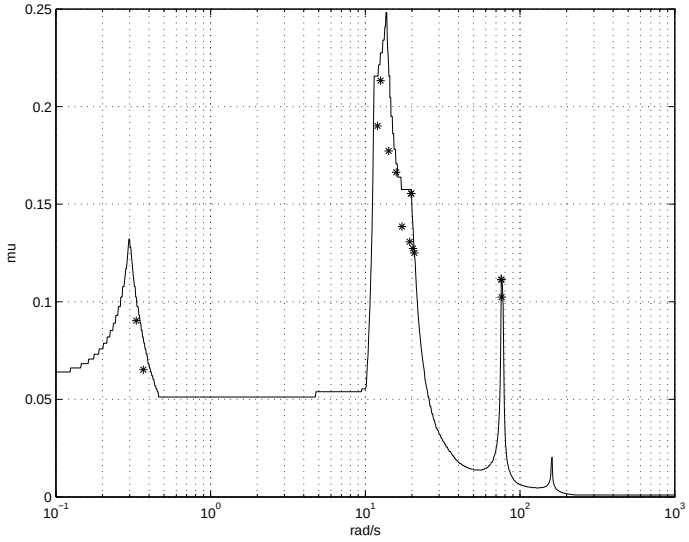

Figure 11: μ for the missile example (robust stability inside a truncated sector).

Misleading conclusions may be drawn with *mu_lb_with_freq.m*. To illustrate this let's go back to section 7.2. Figure 10 corresponds to the exponential-time μ upper bound on a frequency gridding (the zero frequency + 100 points between 0.1 and 1000 rad/s + 30 additional points),

noting that the same problem occurs with the mixed μ upper bound. The stars correspond to μ lower bounds computed with $mu\_lb\_with\_freq.m$ (20 points between 0.1 and 1000 rad/s and the zero frequency - 4th method). The μ lower bound seems greater than the μ upper bound around 80 rad/s! This is due to the use of a frequency gridding. Indeed, when refining the frequency gridding around the secondary peak the problem disappears: see figure 11.

10 Telescope mock-up: robust stability

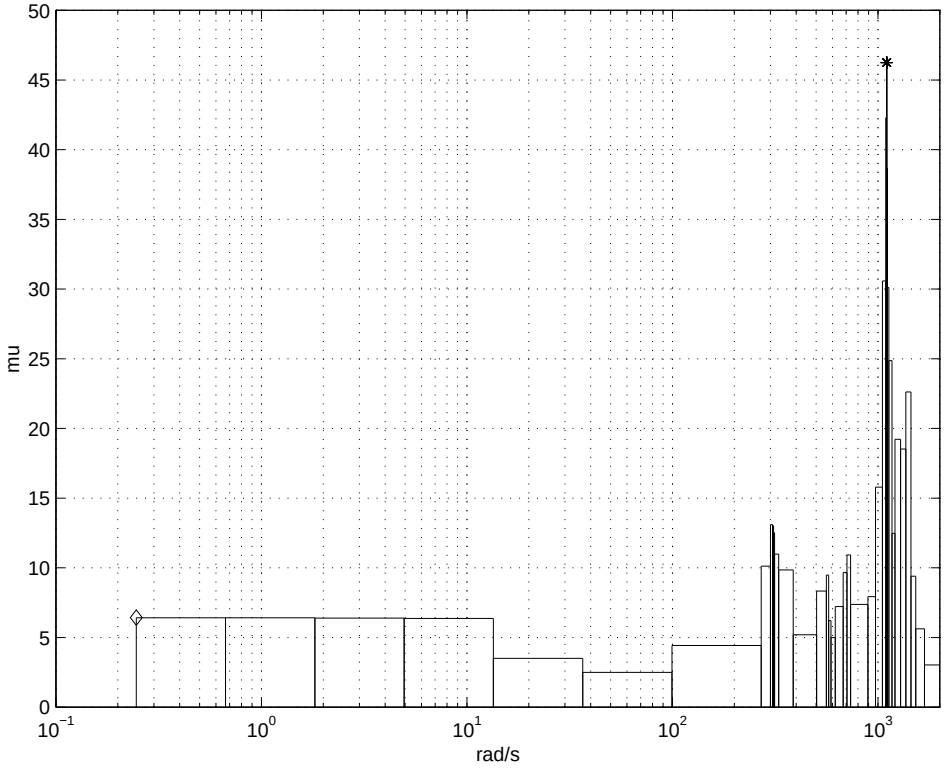

Figure 12: μ for the telescope mock-up example.

The above figure presents the application of $mu\_max\_1.m$ to the telescope mock-up example. The initial frequency gridding only consists of the zero frequency and 10 points between 0.1 and 2000 rad/s. This very rough gridding is then refined inside the routine. Note the very fine peaks on the μ plot. Note also that since it is impossible to directly represent on a logarithmic axis a guaranteed μ upper bound β on the frequency interval [0, 0.1 rad/s], a diamond is simply plotted at the point (0.1, β).

The maximal value is obtained as 46.557 between 1101.019 rad/s and 1103.489 rad/s. This means that robust stability inside the LHP is guaranteed for $\pm$ 2 % of uncertainty in the frequencies of the bending modes ($0.0215 = \frac{1}{46.557}$). A μ lower bound is then computed by applying $mu\_lb\_with\_freq.m$ on the critical frequency interval (10 points between 1101.019 rad/s and 1103.489 rad/s - 4th method). A μ lower bound is obtained as 46.253 at omega = 1103.309 rad/s (see the star on the figure). maximal μ lower and upper bounds nearly coincide.

11 Missile: skew μ problems

11.1 Robust stability in the presence of parametric uncertainties and neglected dynamics

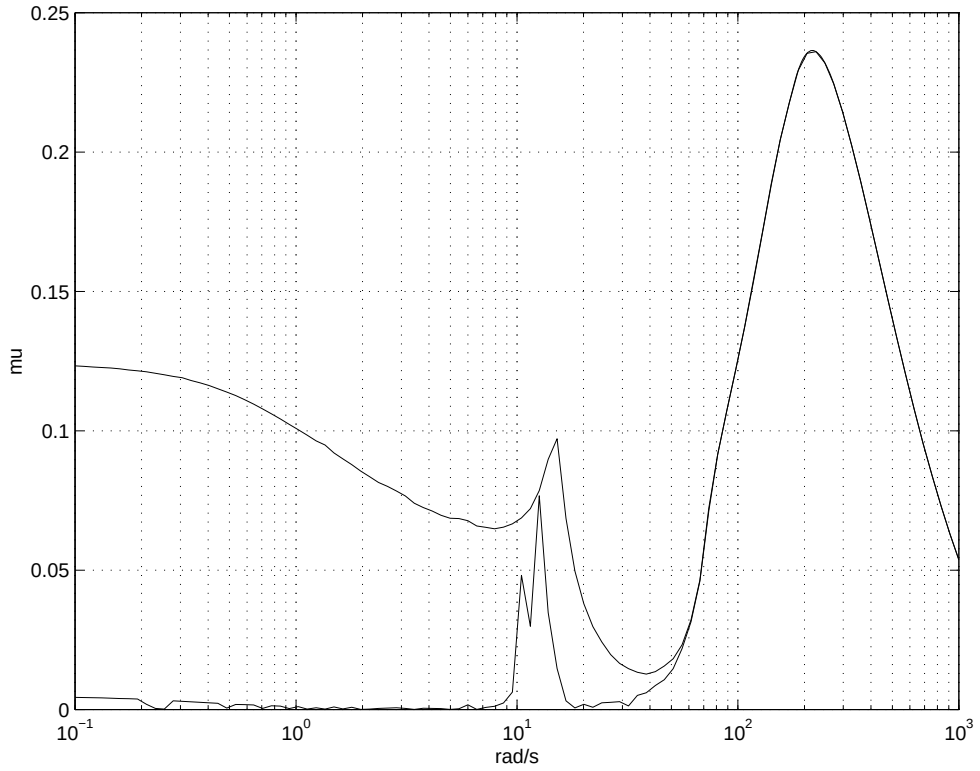

Figure 13: μ for the missile example (robust stability).

We now go back to the missile example. In this subsection one studies robust stability in the LHP, in the presence of parametric uncertainties and neglected dynamics. Robust stability is first analysed with the μ tool (see figure 13; the upper curve is the mixed μ upper bound, the lower one is the mixed μ lower bound). The maximal value of the mixed μ upper bound is 0.236 at 216.552 rad/s, so that the maximal uncertainty in the stability derivatives is $5/0.236 = 21.18\%$ (remember the weighting factor on the parametric uncertainties is 5 %). The result is nearly non-conservative, because of the very small gap between the μ lower and upper bounds at the critical frequency (lower and upper bounds nearly coincide at high frequencies).

However, the controller must tolerate a given amount of neglected dynamics, as defined by the template. It is thus logical to maintain this uncertainty inside its unit ball in our analysis

problem. The maximal value of the mixed skew μ upper bound is obtained as 0.125 at the zero frequency, so that the maximal uncertainty in the stability derivatives becomes $5/0.125 = 40\%$ (see figure 14).

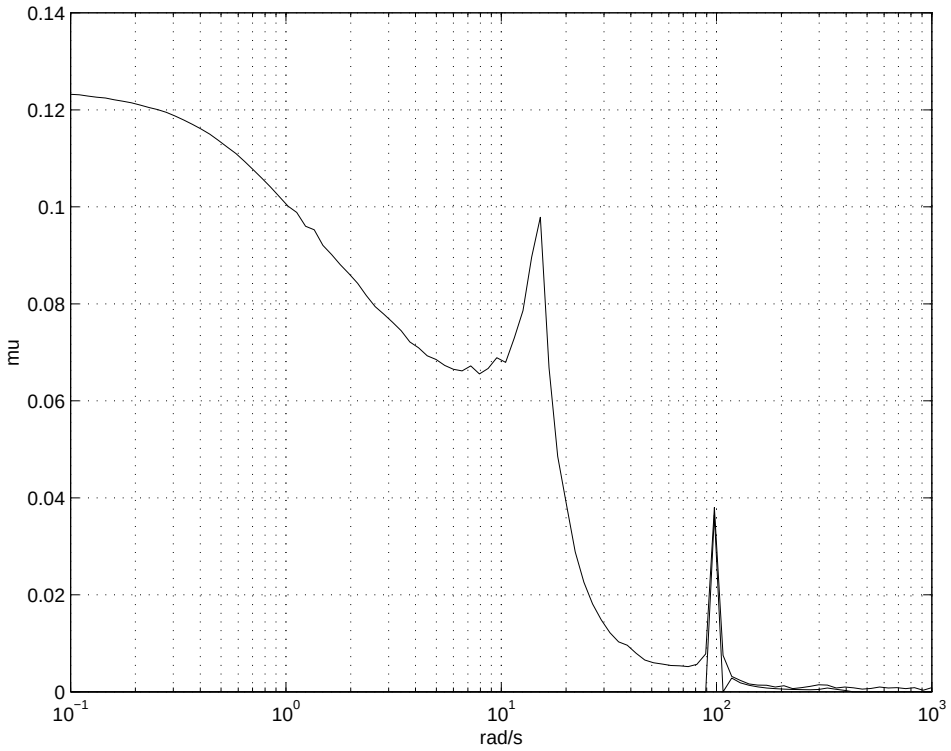

Figure 14: skew μ for the missile example (robust stability).

More precisely, figure 13 also presents the mixed μ lower bound provided by the power algorithm in the μ Analysis and Synthesis Toolbox, while figure 15 presents the mixed μ lower bound provided by our power algorithm for the same problem. The result of these 2 figures is not really satisfactory. In the same way figure 14 presents the mixed skew μ lower bound provided by our power algorithm. Here again the result is not satisfactory. Nevertheless, the mixed μ problem of this section is very close to a real μ one at low and middle frequencies, so that the power algorithms logically fail to converge at these frequencies. Much better results are obtained in the next subsection, which corresponds to a true mixed μ problem.

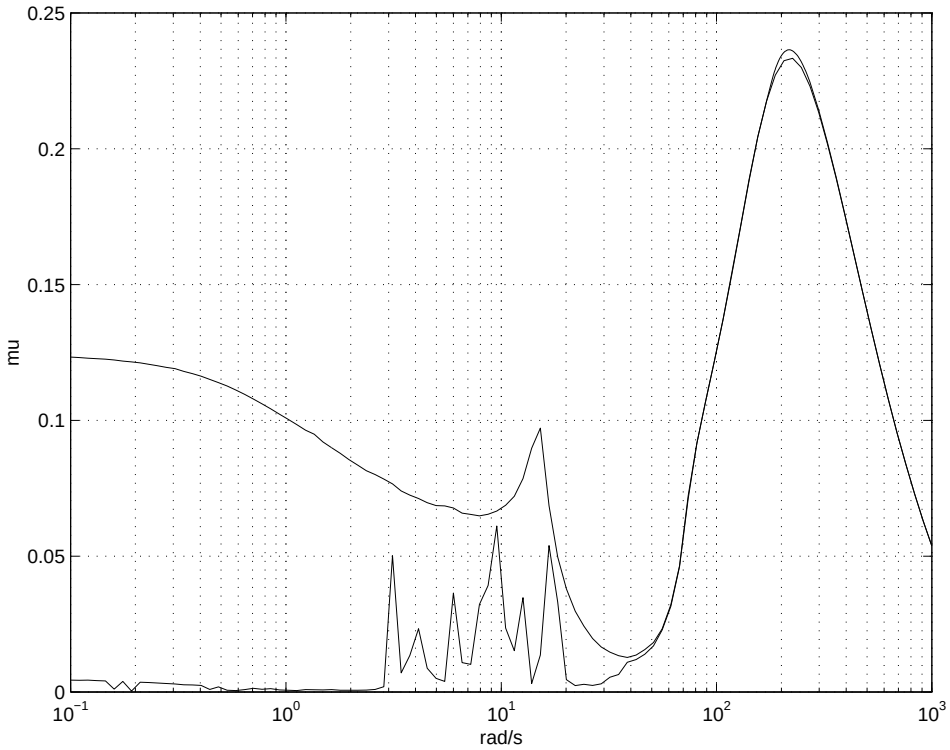

Figure 15: μ for the missile example (robust stability).

11.2 Robust performance

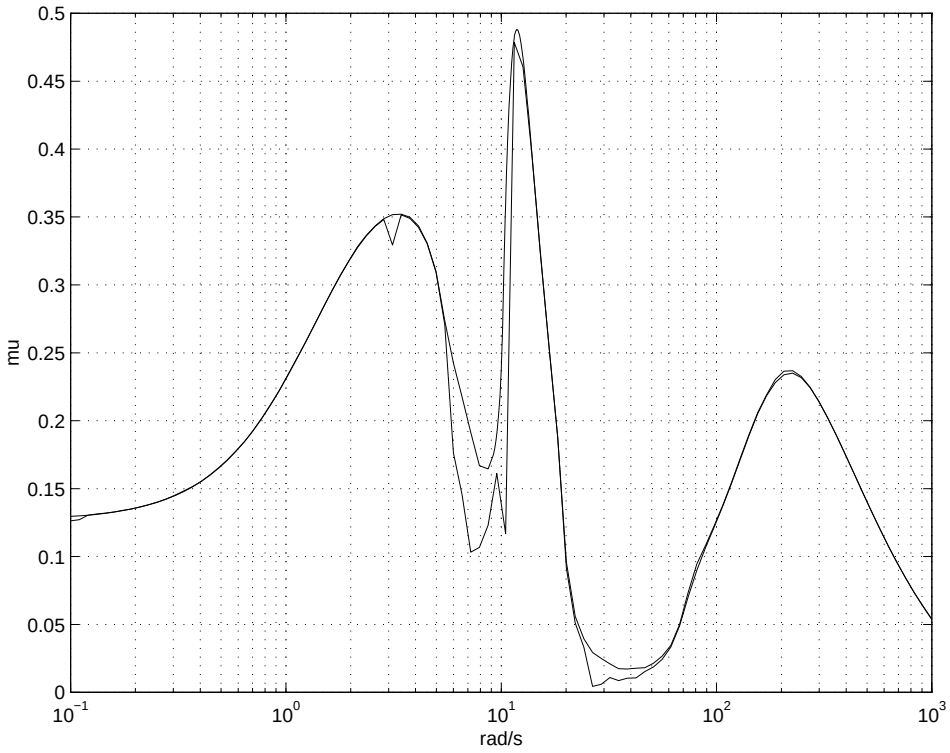

Figure 16: skew μ for the missile example (robust performance).

The issue is to compute the maximal amount of model uncertainties (parametric uncertainties and neglected dynamics), for which the frequency-domain template on the sensitivity function $S(s)$ is still satisfied. The mixed skew μ upper bound is computed as a function of frequency in the above figure (the lower curve corresponds to the skew mixed μ lower bound). The maximal value is obtained as 0.488 at 11.830 rad/s. The result is quite satisfactory, since the lower and upper bounds nearly coincide at this frequency. Robust performance is thus guaranteed for $\pm$ 10 % of uncertainties in the stability derivatives ($0.102 = \frac{0.05}{0.488}$).

Note that the skew μ lower bound is rather satisfactory in the above figure. When applying classical μ tools to the same problem the two following figures are obtained, either with the power algorithm in the μ Analysis and Synthesis Toolbox, or with ours[4]. The results provided by both power algorithms are quite satisfactory.

[4]More precisely *mu_frequency_gridding.m* uses *mixed_mu_lb_freq.m*, which itself calls *mixed_mu_lb.m*.

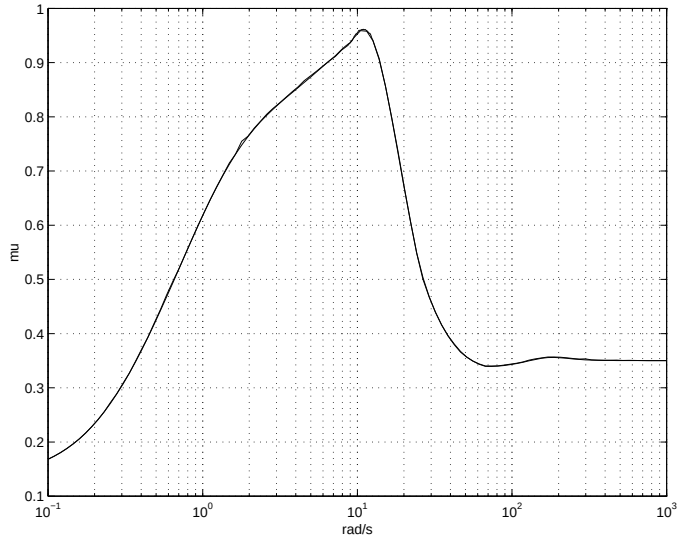

Figure 17: μ for the missile example (robust performance).

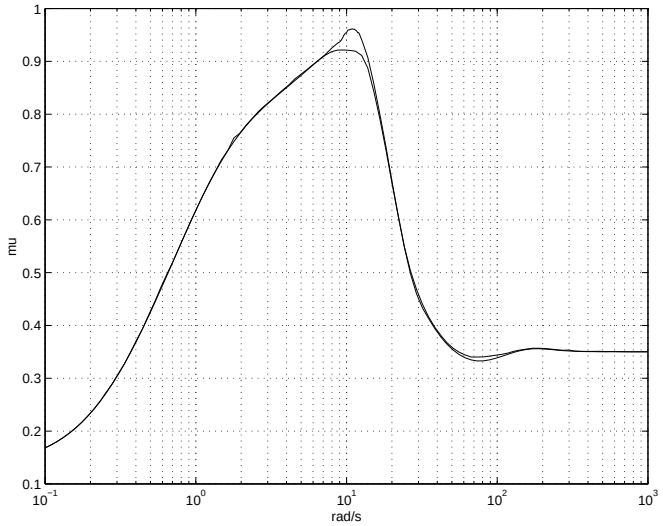

Figure 18: μ for the missile example (robust performance).

12 Computation of robust gain, phase and delay margins

Consider again the closed loop missile system of figure 4, without the block Δ_2 of neglected dynamics, i.e. one just keeps the 4 parametric uncertainties in Δ_1. An uncertain time-delay (or gain or phase) is introduced at the plant input, and 2 other time-delays (or gains or phases) are introduced at the 2 plant outputs.

Let δ the vector of 4 parametric uncertainties. For a given value of δ, let e.g. $\tau(\delta)$ the delay margin associated to the closed loop, i.e. robust stability can be guaranteed for all three time delays belonging to $[0,\ \tau(\delta)]$ (with independent variations). The worst-case delay margin is defined as $\min_{\delta \in D} \tau(\delta)$, i.e. the worst case value of the margin when δ belongs to the unit hypercube D (see equation (14) for a definition of D). Worst-case gain and phase margins are defined in the same way.

A small gain approach is used, as detailed in [5]. A skew μ problem is to be solved. Nevertheless, in this reference, if the phase margin is $[-A,\ A]$ at a frequency ω, the delay margin is deduced as $[-A/\omega,\ A/\omega]$. The present toolbox proposes an improved solution, in which the delay margin corresponds to an interval $[0,\ \tau_{max}]$. To this aim, if the initial delay margin was computed as $[-A/\omega,\ A/\omega]$, fixed time-delays $e^{-jA/2}$ are added to the nominal closed loop at frequency ω, and the small gain theorem is once again applied (more precisely a skew μ problem is once again to be solved). To reduce the computational burden this is done only at critical frequencies, where the delay margin is the smallest.

Remarks:
(*i*) More generally it is possible to compute worst-case margins in the presence of a mixed model perturbation Δ which is maintained inside its unit ball.
(*ii*) In the following *demo_delays.m* calls the main routine *worst_case_margin.m*, which itself calls *skew_mu_ub_bis.m* or *mu_ub.m*. See the help of *worst_case_margin.m*.

We first compute with *demo_delays.m* estimates of the gain, phase and delay margins in the case of the nominal closed loop, without parametric uncertainties. The following result is obtained:

```
w = 35.232 rad/s --> worst-case phase margin = 18.388 degrees

w = 82.143 rad/s --> worst-case delay margin = 6.326e-03 s

w = 25.826 rad/s --> worst-case lower gain margin =  0.690

w = 47.138 rad/s --> worst-case upper gain margin =  1.448
```

Using our improved technique it is then possible to increase the delay margin up to 8.270e-03 s (the minimal value of the margin over frequency is now obtained at 47.138 rad/s), i.e. a

significant increase of 24 % with a low additional computational burden.

demo_delays_bis.m is used to compute a destabilizing value of the delays (still without parametric uncertainties). A sinusoidal response is obtained for 9.7 ms, an unbounded one for 9.8 ms. More precisely this worst-case corresponds to 9.8 ms for the delay at the plant input, 0 s for the delay at the first plant output, and 9.8 ms for the delay at the second plant output. Note the reasonable gap between the lower and upper bounds of the delay margin (14.7 % between 8.27 ms and 9.7 ms). The gap corresponding to the non-improved delay margin is much higher (35 % between 6.326 ms and 9.7 ms). This suggest that with our improved technique, the use of the small gain theorem is not especially conservative.

We now compute the worst-case gain, phase and delay margins, when parametric uncertainties vary between ± 15 % (remember the robust stability margin is about 40 %). The following result is obtained:

```
w = 14.829 rad/s --> worst-case phase margin = 16.236 degrees

w = 78.428 rad/s --> worst-case delay margin = 5.566e-03 s

w = 17.028 rad/s --> worst-case lower gain margin =  0.737

w = 14.829 rad/s --> worst-case upper gain margin =  1.394
```

It is then possible to increase the worst-case delay margin up to 7.762e-03 s (the minimal value of the margin over frequency is now obtained at 49.370 rad/s), i.e. a significant increase of 28 % with a low additional computational burden.

References

[1] R.L. Dailey. A new algorithm for the real structured singular value. *Proceedings of the ACC*, pages 3036–3040, 1990.

[2] R.R.E. DeGaston and M.G. Safonov. Exact calculation of the multiloop stability margin. *IEEE Transactions on Automatic Control*, 33(2):156–171, 1988.

[3] J. Doyle. Analysis of feedback systems with structured uncertainties. *IEE Proceedings, Part D*, 129(6):242–250, 1982.

[4] M.K.H. Fan, A.L. Tits, and J.C. Doyle. Robustness in the presence of mixed parametric uncertainty and unmodeled dynamics. *IEEE Transactions on Automatic Control*, 36(1):25 – 38, 1991.

[5] G. Ferreres. *A practical approach to robustness analysis with aeronautical applications.* Kluwer Academic/Plenum Publishers, 1999.

[6] G. Ferreres and J.M. Biannic. A μ analysis technique without frequency gridding. *Proc. of the ACC*, 4:2294–2298, 1998.

[7] G. Ferreres and J.M. Biannic. Reliable computation of the robustness margin for a flexible transport aircraft. *Control Engineering Practice*, 9:1267–1278, 2001.

[8] G. Ferreres and V. Fromion. Computation of the robustness margin with the skewed μ tool. *Systems and Control Letters*, 32(4):193–202, December 1997.

[9] G. Ferreres, J.F. Magni, and J.M. Biannic. Robustness analysis of flexible structures: practical algorithms. *International Journal of Robust and Nonlinear Control*, 13:715–734, 2003.

[10] J-F. Magni. Linear Fractional Representation Toolbox for use with Matlab. - Free Web publication - *http://www.cert.fr/dcsd/idco/perso/Magni/mypage.html*, 2001.

[11] M.P. Newlin and S.T. Glavaski. Advances in the computation of the μ lower bound. *Proceedings of the ACC*, pages 442–446, 1995.

[12] R.T. Reichert. Dynamic scheduling of modern robust control autopilot design for missiles. *IEEE Control System Magazine*, 12(5):35–42, October 1992.

[13] M.G. Safonov. Stability margins of diagonally perturbed multivariable feedback systems. *IEE Proceedings, Part D*, 129(6):251–256, 1982.

[14] P.M. Young and J.C. Doyle. Computation of μ with real and complex uncertainties. *Proceedings of the IEEE CDC*, pages 1230–1235, 1990.

[15] L.A. Zadeh and C.A. Desoer. *Linear system theory.* McGraw-Hill, New York, 1963.